





Bulk contributions to the Casimir interaction of Dirac materialsM. Bordag ^{1,*}, I. Fialkovsky ², N. Khusnutdinov ^{2,†} and D. Vassilevich ^{2,3,‡}¹*Leipzig University, Institute for Theoretical Physics, 04109 Leipzig, Germany*²*CMCC-Universidade Federal do ABC, Santo André, S.P. CEP 09210-580, Brazil*³*Physics Department, Tomsk State University, Tomsk 634050, Russia*

(Received 28 July 2021; revised 18 October 2021; accepted 17 November 2021; published 29 November 2021)

Exploiting methods of quantum field theory we compute the bulk polarization tensor and bulk dielectric functions for Dirac materials in the presence of a mass gap, chemical potential, and finite temperature. Using these results (and neglecting eventual boundary effects), we study the Casimir interaction of Dirac materials. We describe in detail the characteristic features of the dielectric functions and their influence on the Casimir pressure.

DOI: [10.1103/PhysRevB.104.195431](https://doi.org/10.1103/PhysRevB.104.195431)**I. INTRODUCTION**

Topological insulators [1,2] are among the most interesting and most actively studied materials of modern condensed matter physics. The characteristic feature of these materials is the presence of topologically protected surface states. [We shall consider here three-dimensional (3D) materials only]. The simplest continuous model having this property is a massive Dirac fermion subjected to suitable boundary conditions.

Over the recent years, the physics of the Casimir interaction [3] emerged as an important instrument for the study of properties of new materials [4,5]. First of all, the Casimir effect is an integral effect which depends on the properties of the dielectric functions at all frequencies and all momenta. Such properties are hard to analyze with other methods. Besides, the Casimir interaction dominates at short separations. Thus, the study of the Casimir force is important for applications in nanoelectromechanical systems. The main tool for our study is the fermion polarization tensor. Because of its high complexity it is useful to study its bulk contribution separately and to postpone the inclusion of the remaining parts. The present work is dedicated to the bulk part. The effects of surface states will be neglected.

The materials which we consider in this paper have a nonzero mass gap in the bulk (like the topological insulators, e.g.). Thus zero-gap Dirac semimetals are not included. Also, we do not consider Weyl semimetals which are characterized by a nonzero separation between Weyl points in the momentum space. We briefly comment on possibilities to include these very interesting materials in our approach in Sec. V. The publications on the Casimir interactions of various Dirac materials have been reviewed in Refs [4,5]. We make mention of a couple of recent papers, Refs. [6–8]. The papers which have been published so far use different physical setups. A detailed comparison of our approach to that of the current literature is postponed to Sec. V.

The bulk electronic properties will be expressed in terms of the polarization tensor of Dirac fermions and computed using the methods of quantum field theory (QFT) as a one-loop Feynman diagram. This approach was applied to a 2D Dirac material — graphene — in the papers [9,10] and subsequently confirmed in the experimental studies [11–13]. The polarization tensor approach is known to take properly into account the spatial dispersion effects by construction. As it has been demonstrated recently [14,15], these effects are essential for a resolution of some internal controversies in the Casimir physics. To describe a wide range of materials we need the full expression for the polarization tensor at arbitrary values of four-momenta, mass m , temperature T , and chemical potential μ . Despite the large literature on finite-temperature QFT we were not able to find a suitable expression of the required level of generality and had to redo this (rather standard) calculation. For example, in the papers [16–20] just the polarization function rather than the full polarization tensor was computed. Also, even the polarization function was not given for the whole range of parameters which we need in our work. The dielectric functions ε^l (longitudinal) and ε^t (transversal) are expressed through components of the polarization tensor with the help of Lindhard formalism [21]. We mention closely related calculations in Ref. [22]. There the Casimir interaction between half-spaces with a scalar field confined to them, interacting through another scalar field across the gap, was calculated using the TGTG-formula¹. However, the methods for the calculation of the polarization tensor used there, are different from the ones used in the present paper.

Our purpose is not to study the Casimir interaction of a particular material, but rather to answer the question: What are the characteristic features of dielectric functions and the Casimir pressure of a material having Dirac quasiparticles in the bulk? Therefore, we perform our study for a reasonably wide range of parameters. We find that quantum corrections

*bordag@uni-leipzig.de

†nail.khusnutdinov@gmail.com

‡dvassil@gmail.com

¹TGTG is a shorthand notation for Green's function - T-matrix - Green's function - T-matrix in the scattering approach to the Casimir effect.

to the magnetic permeability are always negligible. The dielectric functions $\epsilon^{l,t}$ have a strong peak at low (imaginary) frequencies and momenta with rather characteristic dependence on m , μ , and T , and a slow varying tail at moderate or high momenta and frequencies. The Casimir pressure between two identical Dirac materials is influenced significantly by quantum corrections. It is suppressed at short distances and low temperatures and enhanced at large separations and high temperatures. We trace this behavior back to the properties of dielectric functions. We also find that almost the whole dependence of the Casimir pressure on T and μ is due to the zero Matsubara frequency contribution to the Lifshitz sum.

In this work, we neglect the effects of impurities and well as the contributions to the polarization tensor from the fermionic surface states. It is hard to make any definite conclusions on the relative amplitude of these effects before explicit calculations have been performed. (We postpone them to a future work.) There are, however, some indirect arguments implying that our model should indeed be a good approximation to a realistic situation. They are based on a comparison to the Casimir interaction of graphene, which is the only Dirac material whose Casimir interaction has been studied experimentally (see Refs. [11–13]). First, the experiment shows a good agreement with the theory based on a polarization tensor computed without taking into account the contributions of impurities. Thus, it is reasonable to neglect the effects of impurities of other Dirac materials as well (at least in the first approximation and if they are clean enough). Note, that the influence of impurities on the Casimir force has never been studied in the approach based on polarization tensor. Second, the effects of surface states for 3D materials can be mimicked by a sheet of graphene on top of a dielectric. Both theory and experiment in this case show that the main contributions to the Casimir force comes from the dielectric bulk. This can be related to differences in the dependence of polarization tensor on the Fermi velocity in 3+1 and 2+1 dimensions, see discussion in the next section. Thus, neglecting surface states in the first approximation is not so unreasonable.

This paper is organized as follows. The polarization tensor is computed in the next section while some details of this computation are placed in the Appendix. In Sec. III we analyze the dielectric functions at imaginary frequencies. Section IV is dedicated to the Casimir interaction. Some concluding remarks are contained in Sec. V.

Throughout the paper we use natural units $\hbar = c = k_B = 1$, if not stated otherwise.

II. POLARIZATION TENSOR AND ITS FORM FACTORS

We consider an idealized material with quasiparticle excitations corresponding to one generation of Dirac fermions. Their spectrum is described by the Dirac operator

$$\not{D} = i\tilde{\gamma}^\nu(\partial_\nu + ieA_\nu) + m. \quad (1)$$

Here $\nu = 0, 1, 2, 3$ is a four-vector index, A_ν is an electromagnetic potential. A tilde over a four-vector means that the components are rescaled with the Fermi velocity v_F as

$$\tilde{\gamma}^\mu \equiv \eta_v^\mu \gamma^\nu, \quad \eta = \text{diag}(1, v_F, v_F, v_F). \quad (2)$$

The matrices γ^μ satisfy the usual Clifford relation $\gamma^\mu \gamma^\nu + \gamma^\nu \gamma^\mu = 2g^{\mu\nu}$ with $g = \text{diag}(+1, -1, -1, -1)$. Particular

representation of the γ matrices will play no role in what follows. Without any loss of generality we assume $m \geq 0$.

The interaction with quantum fermions leads to the following effective action in quadratic order for the electromagnetic potential:

$$S_{\text{eff}} = \frac{1}{2} \int d^4x d^4y A_\mu(x) \Pi^{\mu\nu}(x, y) A_\nu(y), \quad (3)$$

where $\Pi^{\mu\nu}$ is the polarization tensor. Due to the translation invariance, it is convenient to make a Fourier transformation in Eq. (3). Our conventions are clear from the formula

$$A_\mu(x) = \int \frac{d^4k}{(2\pi)^4} e^{ikx} A_\mu(k).$$

Thus, we have

$$S_{\text{eff}} = \frac{1}{2} \int \frac{d^4k}{(2\pi)^4} A_\mu(-k) \Pi^{\mu\nu}(k) A_\nu(k). \quad (4)$$

For zero temperature and zero chemical potential, $T = \mu = 0$, and to the lowest order of perturbation expansion (one-loop) the polarization tensor, which will be denoted by $\Pi_0(k)$, can be written as

$$\Pi_0^{\mu\nu}(p) = ie^2 \int \frac{d^4k}{(2\pi)^4} \text{tr} [\tilde{\gamma}^\mu \not{D}_0^{-1}(k) \gamma^\nu \not{D}_0^{-1}(k-p)]. \quad (5)$$

Here $\not{D}_0^{-1}(k)$ is a Fourier transform of the inverse of free Dirac operator ($A_\mu = 0$),

$$\not{D}_0^{-1}(k) = -\frac{k_\mu \tilde{\gamma}^\mu + m}{k^2 - m^2}. \quad (6)$$

We use causal Green's functions, so that the integration contour for k_0 is defined by the shift $k_0 \rightarrow k_0 + i0 \text{sgn}(k_0)$.

To include a nonzero temperature T and a nonzero chemical potential μ we shall use the imaginary time Matsubara formalism. First, one has to shift the temporal components of the momenta of fermions by the chemical potential μ , $k_0 \rightarrow k_0 + \mu$, without shifting the contour. Then one has to introduce imaginary Matsubara frequencies, $k_0 \rightarrow ik_4$, $p_0 \rightarrow ip_4$, $k_4 = 2\pi T(n + \frac{1}{2})$, $p_4 = 2\pi Tl$, $n, l \in \mathbb{Z}$. (Later we shall use a special notation $\xi_l = 2\pi lT$ for the bosonic Matsubara frequencies). At the last step, one has to replace the integral over k_0 by a sum over the Matsubara frequencies,

$$\int_{-\infty}^{\infty} dk_0 \rightarrow 2\pi iT \sum_{n \in \mathbb{Z}}. \quad (7)$$

Thus, we obtain

$$\Pi^{\mu\nu}(p) = -e^2 T \sum_{n \in \mathbb{Z}} \int \frac{d^3\vec{k}}{(2\pi)^3} \text{tr} [\tilde{\gamma}^\mu S(k) \tilde{\gamma}^\nu S(k-p)], \quad (8)$$

where all momenta are Euclidean as described above. $S(k)$ is the Euclidean propagator,

$$S(k) = -\frac{(ik_4 + \mu)\gamma^0 + v_F \vec{k} \times \vec{\gamma} + m}{(ik_4 + \mu)^2 - v_F^2 \vec{k}^2 - m^2}. \quad (9)$$

Our notations respect the natural position of indices, $\vec{k} = (k_1, k_2, k_3)$ while $\vec{\gamma} = (\gamma^1, \gamma^2, \gamma^3)$. We stress that we do not change the γ matrices and do not make Euclidean rotation of the components of $\Pi^{\mu\nu}$.

As we know, see for example Ref. [23], the dependence of Π on the Fermi velocity can be accounted for in a very simple way. One can make the change of integration variable $\vec{k} \rightarrow v_F \vec{k}$ in (8) to see that

$$\Pi^{\mu\nu}(p) = v_F^{-3} \eta_\rho^\mu \eta_\sigma^\nu \widehat{\Pi}^{\rho\sigma}(\vec{p}), \quad (10)$$

where $\widehat{\Pi}^{\mu\nu}(p)$ is the polarization tensor computed for $v_F = 1$ and $\vec{p}_\mu = \eta_\mu^\nu p_\nu$. As we shall see below, to reconstruct full tensor structure one needs just two specific combinations of the components of $\widehat{\Pi}^{\mu\nu}$, namely $\widehat{\Pi}^{00}$ and $\widehat{\Pi}^{\text{tr}} \equiv \widehat{\Pi}_\mu^\mu$. We introduce a shorthand notation $\widehat{\Pi}^{\mathbf{x}}$ for both of them with either $\mathbf{x} = 00$ or $\mathbf{x} = \text{tr}$.

In $2 + 1$ dimensions, an analog of Eq. (10) contains a factor of v_F^{-2} instead of v_F^{-3} . This suggest that bulk quantum effects are more important than the effects of surface states.

The computations of polarization tensor can be found in the Appendix, the final result reads

$$\widehat{\Pi}^{\mathbf{x}}(p) = \widehat{\Pi}_0^{\mathbf{x}}(p) + \widehat{\Pi}_{T,\mu}^{\mathbf{x}}(p), \quad (11)$$

where individual terms on the right-hand side are given by

$$\widehat{\Pi}_{T,\mu}^{\mathbf{x}}(p) = + \frac{e^2}{2\pi^2} \int_0^\infty \frac{\vec{k}^2 d|\vec{k}|}{E_k} \{I_+^{\mathbf{x}} + I_-^{\mathbf{x}}\} \Xi(E_k, \mu), \quad (12)$$

$$\widehat{\Pi}_0^{\mathbf{x}}(p) = - \frac{e^2}{2\pi^2} \int_0^\infty \frac{\vec{k}^2 d|\vec{k}|}{E_k} \{I_+^{\mathbf{x}} + I_-^{\mathbf{x}}\}. \quad (13)$$

We used the following notations:

$$\Xi(E_k, \mu) = \frac{1}{e^{\frac{E_k+\mu}{T}} + 1} + \frac{1}{e^{\frac{E_k-\mu}{T}} + 1}, \quad E_k = \sqrt{m^2 + \vec{k}^2}, \quad (14)$$

and

$$I_\pm^{00} = 1 + \frac{4E_k^2 - \vec{p}^2 - p_4^2 \pm 4ip_4 E_k}{4|\vec{k}||\vec{p}|} \ln \left[\frac{\vec{p}^2 + p_4^2 + 2|\vec{k}||\vec{p}| \mp 2ip_4 E_k}{\vec{p}^2 + p_4^2 - 2|\vec{k}||\vec{p}| \mp 2ip_4 E_k} \right],$$

$$I_\pm^{\text{tr}} = 2 \left\{ 1 + \frac{2m^2 - \vec{p}^2 - p_4^2}{4|\vec{k}||\vec{p}|} \ln \left[\frac{\vec{p}^2 + p_4^2 + 2|\vec{k}||\vec{p}| \mp 2ip_4 E_k}{\vec{p}^2 + p_4^2 - 2|\vec{k}||\vec{p}| \mp 2ip_4 E_k} \right] \right\}. \quad (15)$$

A characteristic property of the split (11) is that the tensor $\widehat{\Pi}_0$ depends neither on T , nor on μ , while the part $\widehat{\Pi}_{T,\mu}$ vanishes when $T = \mu = 0$. This motivates our choice of notations. The representation (11) has many other advantages which will be explained below.

Let us now show how the full expression for polarization tensor can be recovered from $\widehat{\Pi}^{\text{tr}}$ and $\widehat{\Pi}^{00}$. The polarization tensor for the problem in question has to satisfy a number of symmetry requirements. It has to be symmetric, invariant under spatial rotations and transversal. Thus, just two independent tensor structures are allowed:

$$\Pi^{\mu\nu}(p) = \varphi_L(p) P_L^{\mu\nu} + \varphi_T(p) P_T^{\mu\nu}, \quad (16)$$

$$P_L^{\mu\nu} = \frac{p^\mu p^\nu}{p^2} - \frac{p^\mu u^\nu + p^\nu u^\mu}{p_0} + \frac{u^\mu u^\nu p^2}{p_0^2}, \quad P_T^{\mu\nu} = g^{\mu\nu} - \frac{p^\mu p^\nu}{p^2},$$

where $u = (1, 0, 0, 0)$ in the medium rest reference frame. The scalar functions φ_L and φ_T (form factors) can be expressed through the components of polarization tensor as

$$\varphi_T = \frac{1}{2} \left(\frac{p^2}{\vec{p}^2} \Pi^{00} + \Pi_\mu^\mu \right), \quad \varphi_L = \frac{p_0^2}{2\vec{p}^2} \left(\frac{3p^2}{\vec{p}^2} \Pi^{00} + \Pi_\mu^\mu \right). \quad (17)$$

By using Eq. (10) we can express these quantities through the polarization tensor at $v_F = 1$,

$$\Pi^{00}(p) = v_F^{-3} \widehat{\Pi}^{00}(\vec{p}), \quad \Pi_\mu^\mu(p) = v_F^{-3} (1 - v_F^2) \widehat{\Pi}^{00}(\vec{p}) + v_F^{-1} \widehat{\Pi}_\mu^\mu(\vec{p}). \quad (18)$$

Equations (17) and (18) are valid for both terms of the split (11) Π_0 and $\Pi_{T,\mu}$ individually.

The integral over $|\vec{k}|$ in Eq. (13) is divergent. Thus the polarization tensor $\Pi^{\mu\nu}$ needs to be regularized and renormalized. Note that $\Pi_{T,\mu}$ is finite, so that the renormalization can be performed at zero temperature and zero chemical potential, as expected. In the presence of v_F , the renormalization was performed recently in Ref. [23] in the Pauli-Villars formalism which we follow in this work (see also Refs. [24–27] for a renormalization group analysis of such theories). A short summary of the procedure used in Ref. [23] is as follows. One uses subtraction of the contributions of Pauli-Villars regulator fields to polarization tensor. The expressions obtained are still divergent in the limit of infinitely massive regulators. These divergences are removed by a redefinition of bare dielectric permittivity ε_0 and magnetic permeability $\mu_{M,0}$ in the Maxwell action in a media

$$S_M = \frac{1}{2} \int \frac{d^4 p}{(2\pi)^4} [\varepsilon_0 \vec{E}(-p) \times \vec{E}(p) - \mu_{M,0}^{-1} \vec{B}(-p) \times \vec{B}(p)]. \quad (19)$$

According to the general philosophy of renormalization, ε_0 and $\mu_{M,0}$ do not depend on the momentum p . These two constants cannot be predicted in the framework of QFT and have to be considered as an input. The *renormalized* Π_0 reads

$$\Pi_0^{\mu\nu}(p) = - \frac{e^2}{2\pi^2 v_F^3} \eta_\sigma^\mu \eta_\rho^\nu [\vec{p}^\sigma \vec{p}^\rho - g^{\sigma\rho} \vec{p}^2] f(\vec{p}^2/m^2), \quad f(z) \equiv \int_0^1 dx x(1-x) \ln[1 - zx(1-x)]. \quad (20)$$

To avoid a notation clutter, we do not introduce any special symbol for the renormalized tensor. From now on, only renormalized quantities will be used. $f(0) = 0$, and thus ε_0 , and $\mu_{M,0}$ can be interpreted as a dielectric permittivity and a magnetic permeability, respectively, they are measured at vanishing temperature, zero chemical potential and zero external momentum. The quantum effective action (4) obtained in this way vanishes in the limit of infinitely large mass gap, $m \rightarrow \infty$, which is very natural from the physical point of view.

We use now the analysis by Lindhard [21] to relate these quantities to the components of dielectric tensor ε^l and ε^t which are more common in the condensed matter context. The matrix-valued dielectric function ε_{ij} which relates \vec{E} to the electric displacement \vec{D} , $D_i = \varepsilon_{ij}E_j$, can be written through two scalar functions as

$$\varepsilon_{ij}(p) = \left(\delta_{ij} - \frac{p_i p_j}{\vec{p}^2} \right) \varepsilon^l(p) + \frac{p_i p_j}{\vec{p}^2} \varepsilon^t(p). \quad (21)$$

By comparing the standard Maxwell equations to the one obtained by varying $S_M + S_{\text{eff}}$ one comes to the following relations:

$$\varepsilon^l = \varepsilon_0 + \frac{1}{p^2} \left(\frac{\vec{p}^2}{p_0^2} \varphi_L - \varphi_T \right) = \varepsilon_0 + \frac{\Pi^{00}}{\vec{p}^2}, \quad (22)$$

$$\varepsilon^t = \varepsilon_0 - \frac{\vec{p}^2}{p_0^2} \left(\frac{1}{\mu_{M,0}} - 1 \right) - \frac{\varphi_T}{p_0^2} = \varepsilon_0 - \frac{\vec{p}^2}{p_0^2} \left(\frac{1}{\mu_{M,0}} - 1 \right) - \frac{1}{2p_0^2} \left(\frac{p^2}{\vec{p}^2} \Pi^{00} + \Pi_\mu^\mu \right). \quad (23)$$

$$\varepsilon^t(p) = \varepsilon_0 + \frac{\vec{p}^2}{p_4^2} \left(\frac{1}{\mu_{M,0}} - 1 \right) - \frac{e^2}{2\pi^2} \left(\frac{1}{v_F} + \frac{v_F \vec{p}^2}{p_4^2} \right) f(-|\vec{p}|^2/m^2). \quad (26)$$

At this point, we observe that in the terms representing quantum corrections in Eqs. (25) and (26), the spatial momentum \vec{p} is always multiplied by v_F . This makes the spatial dispersion practically irrelevant except for the zeroth Matsubara frequency $p_4 = \xi_0 = 0$. Therefore, for $p_4 \neq 0$ instead of ε^l and ε^t one can use the dielectric permittivity and magnetic permeability which are given by the formulas [21,28]

$$\varepsilon(p_4) = \lim_{\vec{p} \rightarrow 0} \varepsilon^l(p) = \lim_{\vec{p} \rightarrow 0} \varepsilon^t(p), \quad 1 - \frac{1}{\mu_M} = - \lim_{\vec{p} \rightarrow 0} \frac{p_4^2}{\vec{p}^2} (\varepsilon^t - \varepsilon^l), \quad (27)$$

where in all function the Wick rotation $p_0 = ip_4$ is understood. By using Eqs. (20) we obtain

$$\varepsilon(p_4) = \varepsilon_0 - \frac{e^2}{2\pi^2 v_F} f(-p_4^2/m^2), \quad \mu_M^{-1}(p_4) = \mu_{M,0}^{-1} - \frac{e^2 v_F}{2\pi^2} f(-p_4^2/m^2). \quad (28)$$

As compared to quantum corrections $\Delta_0 \varepsilon(p_4) \equiv \varepsilon(p_4) - \varepsilon_0$ the corrections to $\Delta_0 \mu_M^{-1}(p_4) \equiv \mu_M^{-1}(p_4) - \mu_{M,0}^{-1}$ are suppressed with v_F^2 which is a very small quantity. Thus, there is no significant correction to $\mu_{M,0}^{-1}$ for $T = \mu = 0$.

Note that $f(-p_4^2/m^2)$ is a monotonously increasing function of p_4^2 . Asymptotically, it behaves as $p_4^2/(30m^2)$ for small p_4^2 and as $\frac{1}{6} \ln(p_4^2/m^2)$ for large p_4^2 . The log term may look troubling since it grows indefinitely for very large values of p_4 . However, such terms are usual in QFT. They signal the necessity of a resummation of perturbation series. Fortunately, for the applications considered in the present paper this effect is not significant due to the presence of an exponential

These two functions will play the central role in our work. At real frequencies, they define the optical properties of a bulk of a Dirac material. At imaginary frequencies, these functions enter the Lifshitz formula for the Casimir energy.

III. BEHAVIOUR OF THE DIELECTRIC FUNCTIONS

From now on we work with Euclidean momenta only. Let us introduce the following notations for the Euclidean norm of four-vectors

$$|p| := \sqrt{p_4^2 + \vec{p}^2}, \quad |\tilde{p}| := \sqrt{p_4^2 + v_F^2 \vec{p}^2}. \quad (24)$$

Although for $T \neq 0$, within the Matsubara formalism, the momentum p_4 takes only discrete values, $p_4 = 2\pi T l$ [see Eq. (7)], the above expressions are valid for any imaginary frequency, $\omega = ip_4$, and the analysis below will be done for continuous values of p_4 regardless of the temperature.

For the purpose of numerical study, we will need some numerical values for the constants characterizing Dirac materials. As we have already mentioned above, we are not going to stick to any particular material. We shall rather make our choice within some reasonable range. We fix $v_F = (600)^{-1}$. The bare dielectric permittivity ε_0 will be allowed to vary between 2 and 10, the mass will be taken 0.01 or 0.1 eV, while the chemical potential will take values between $\mu = 0$ and $\mu = 0.2$ eV.

First, consider the case $T = 0 = \mu$. By using Eqs. (22), (23) and the explicit form of polarization tensor (20) we obtain

$$\varepsilon^l(p) = \varepsilon_0 - \frac{e^2}{2\pi^2 v_F} f(-|\tilde{p}|^2/m^2), \quad (25)$$

damping in the Lifshitz formula for the Casimir pressure, see Eq. (36) below.

For $\mu \neq 0 \neq T$ the dielectric functions are given by complicated expressions. These expressions are invariant with respect to the replacement $\mu \rightarrow -\mu$. From now on we take $\mu \geq 0$. Most remarkable is the behavior of dielectric permittivity at small (imaginary) frequencies:²

$$\Delta_{T,\mu} \varepsilon(p_4) \simeq \frac{\Omega_\varepsilon^2}{p_4^2}. \quad (29)$$

²We use a notation $\varepsilon = \varepsilon_0 + \Delta_0 \varepsilon + \Delta_{T,\mu} \varepsilon$ consistent with the expansion (11) of polarization tensor.

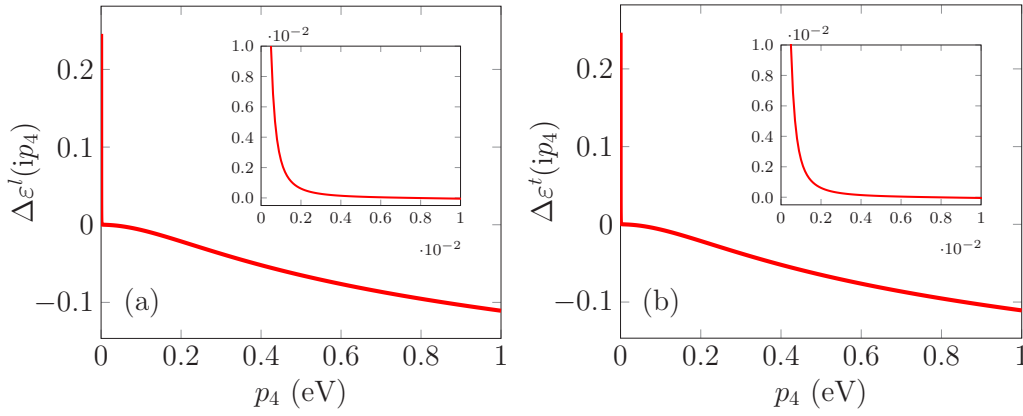


FIG. 1. Total quantum correction $\Delta\varepsilon^{l,t} = \Delta_0\varepsilon^{l,t} + \Delta_T\varepsilon^{l,t}$ as functions of p_4 for $m = 0.1$ eV, $|\vec{p}| = 0.01$ eV, $T = 100$ K, and $\mu = 0$. (a) and (b) represent ε^l and ε^t , respectively.

This term reminds us of the plasma model of dielectric permittivity with the plasma frequency given by

$$\Omega_\varepsilon^2 = \frac{e^2}{3\pi^2 v_F} \int_0^\infty \frac{\vec{k}^2 d|\vec{k}|}{E_k} \frac{2E_k^2 + m^2}{E_k^2} \Xi(E_k, \mu). \quad (30)$$

This integral can be evaluated explicitly in two limiting cases. In the first one, when $\mu < m$ and T is much smaller than $m - \mu$, one has

$$\Omega_\varepsilon^2 \simeq \frac{e^2}{v_F} \sqrt{\frac{mT^3}{2\pi^3}} (e^{-\frac{m-\mu}{T}} + e^{-\frac{m+\mu}{T}}). \quad (31)$$

If $m < \mu$ and $T \ll \mu - m$,

$$\Omega_\varepsilon^2 \simeq \frac{e^2(\mu^2 - m^2)^{3/2}}{3\pi^2 v_F \mu} \left(1 + T^2 \frac{\pi^2}{6} \frac{2\mu^4 + 2m^4 - \mu^2 m^2}{\mu^2(\mu^2 - m^2)^2} \right). \quad (32)$$

In deriving this formula the low-temperature expansion from Ref. [29] is useful.

The correction $\Delta_{T,\mu}\mu_M^{-1}$ for small imaginary frequencies has a form similar to Eq. (29). It is suppressed by a factor of order of v_F^2 as compared to $\Delta_{T,\mu}\varepsilon$. Indeed, as one can check numerically, the corrections to μ_M^{-1} always remain several orders of magnitude smaller than the corrections to ε . This is consistent with the phenomenological observation that Dirac materials are nonmagnetic which also prompts us to use $\mu_{M,0} = 1$ till the end of this paper.

The formula (29) is not valid at the zeroth Matsubara frequency $p_4 = 0$. At this point, the spatial dispersion is not negligible. Thus the full functions ε^l and ε^t have to be considered. The function $\varepsilon^l(0, \vec{p})$ has a pole at $|\vec{p}| = 0$,

$$\varepsilon^l(0, \vec{p}) \simeq \frac{e^2}{\pi^2 v_F^3 \vec{p}^2} \int_0^\infty \frac{d|\vec{k}|}{E_k} \{k^2 + E_k^2\} \Xi(E_k, \mu). \quad (33)$$

If T is much smaller than both m and $|m - \mu|$, the expression above can be simplified as

$$\varepsilon^l(0, \vec{p}) \simeq \frac{e^2}{v_F^3 \vec{p}^2} \sqrt{\frac{mT}{2\pi}} (e^{-\frac{m-\mu}{T}} + e^{-\frac{m+\mu}{T}}) \quad \text{for } m > \mu, \quad (34)$$

$$\varepsilon^l(0, \vec{p}) \simeq \frac{e^2 \mu}{\pi v_F^3 \vec{p}^2} \sqrt{\mu^2 - m^2} \quad \text{for } m < \mu. \quad (35)$$

One sees many similarities to the behavior of the pole term in ε , see Eqs. (29), (30), (32), and (31) above.

The other function ε^t can be analyzed along the same lines. However, due to the structure of reflection coefficients, see Eq. (38) below, the behavior of ε^t at small frequencies and momenta is less important. Typical plots for both ε^l and ε^t are given in Fig. 1. Both graphs have very sharp positive peaks at low frequencies and long slowly-varying negative tails. The peak is so narrow that its influence is practically limited to the zeroth Matsubara frequency.³

IV. CASIMIR INTERACTION

In this section, we study the Casimir interaction between two identical Dirac materials with parallel flat boundaries separated by a vacuum gap a . Let x^3 be the coordinate normal to the boundaries. The Casimir pressure (the force per unit area) is given by the celebrated Lifshitz formula

$$P(a) = -\frac{T}{\pi} \sum_{n=0}^{\infty} \int_0^\infty q_n p_\perp dp_\perp \sum_{l=\text{te,tm}} \left(\frac{e^{2aq_n}}{r_l^2(i\xi_n, p_\perp)} - 1 \right)^{-1}. \quad (36)$$

In the n sum, the Euclidean frequency p_4 takes discrete Matsubara values $p_4 = \xi_n = 2\pi nT$. The prime near the summation symbol means that the term with $n = 0$ enters with a factor of $1/2$. We also defined

$$p_\perp = \sqrt{p_1^2 + p_2^2}, \quad q_n = \sqrt{p_\perp^2 + \xi_n^2}. \quad (37)$$

In Eq. (36), r_{te} and r_{tm} are the reflection coefficients for transverse electric (TE) and transverse magnetic (TM) modes, respectively. To compute the reflection coefficients one needs to know the behavior of the polarization tensor near the boundary. This can be done, at least in principle, by QFT methods as in Refs. [23,30]. However, the computations done in these papers were quite complicated even for zero temperature and zero chemical potential. Thus, in the present work we ignore specific boundary contributions to the polarization tensor and adopt a much simpler approach [31–34] based on the assumption of specular reflection of charged particles at

³For $T = 100$ K the first Matsubara frequency is $\xi_1 = 5.4 \times 10^{-2}$ eV.

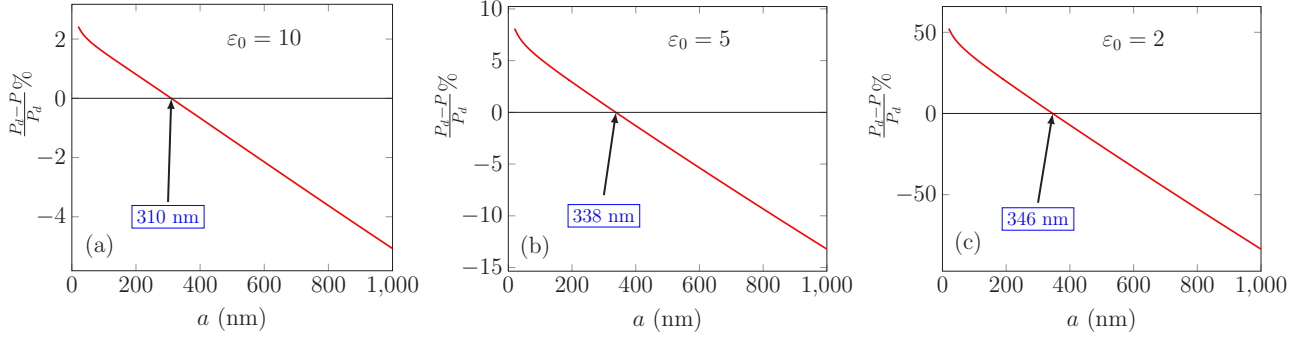


FIG. 2. Relative variation of the Casimir pressure $(P_d - P)/P_d\%$ as a function of separation for $m = 0.01$ eV, $T = 100$ K, $\mu = 0$ and three different values of ε_0 : $\varepsilon_0 = 10, 5,$ and 2 in (a), (b) and (c), respectively.

the boundary. In this approach, the reflection coefficients read

$$\begin{aligned} r_{tm}(i\xi_n, p_\perp) &= \frac{q_n - \xi_n Z_{tm}(i\xi_n, p_\perp)}{q_n + \xi_n Z_{tm}(i\xi_n, p_\perp)}, \\ r_{te}(i\xi_n, p_\perp) &= \frac{q_n Z_{te}(i\xi_n, p_\perp) - \xi_n}{q_n Z_{te}(i\xi_n, p_\perp) + \xi_n}. \end{aligned} \quad (38)$$

The surface impedance functions

$$\begin{aligned} Z_{tm}(i\xi_n, p_\perp) &= \frac{\xi_n}{\pi} \int_{-\infty}^{+\infty} \frac{dp_3}{\bar{p}^2} \left(\frac{p_\perp^2}{\xi_n^2 \varepsilon_n^l} + \frac{p_3^2}{\bar{p}^2 + \varepsilon_n^t \xi_n^2} \right), \\ Z_{te}(i\xi_n, p_\perp) &= \frac{\xi_n}{\pi} \int_{-\infty}^{+\infty} \frac{dp_3}{\bar{p}^2 + \varepsilon_n^t \xi_n^2}, \end{aligned} \quad (39)$$

are completely defined by dielectric functions in the bulk. We used a shorthand notation $\varepsilon_n^{l,t} \equiv \varepsilon^{l,t}(i\xi_n, \bar{p})$.

As a reference point, we will use the Casimir pressure between two identical dielectrics with a constant permittivity ε_0 , i.e., the materials where quantum corrections are neglected. The reflection coefficients in this case read

$$\begin{aligned} r_{te}^{(d)}(i\xi_n, p_\perp) &= \frac{q_n - \sqrt{p_\perp^2 + \varepsilon_0 \xi_n^2}}{q_n + \sqrt{p_\perp^2 + \varepsilon_0 \xi_n^2}}, \\ r_{tm}^{(d)}(i\xi_n, p_\perp) &= \frac{\varepsilon_0 q_n - \sqrt{p_\perp^2 + \varepsilon_0 \xi_n^2}}{\varepsilon_0 q_n + \sqrt{p_\perp^2 + \varepsilon_0 \xi_n^2}}. \end{aligned} \quad (40)$$

To estimate the effect of quantum corrections, let us consider the variation of the Casimir pressure for a Dirac material P relative to the Casimir pressure for dielectrics with a constant permittivity, denoted P_d , plotted as a function of the distance a , Fig. 2, and of the temperature T , Fig. 3. First of all, we see that this relative effect is tiny for $\varepsilon_0 = 10$, considerable for $\varepsilon_0 = 5$, and large for $\varepsilon_0 = 2$. However, this is just a background effect: the pressure P_d used as a reference point increases as a function of ε_0 . The shape of the functional dependence on T is similar to that on a , which confirms the general observation on the Casimir physics: the relevant parameter is the product aT . We see that at large distances and high temperatures quantum corrections increase the Casimir interaction, while for short distances and lower temperatures the interaction decreases.

Qualitatively, the behavior of the Casimir pressure depicted in Figs. 2 and 3 can be explained by the behavior of dielectric

functions described in the previous section. Interestingly, the values of critical temperature, T_c , and critical distance, a_c , defined by $P_d = P$, have a rather weak dependence on ε_0 . Thus, even though the Casimir interaction is a nonlinear effect, the presence of two characteristic regions may be explained by looking at the sign of quantum corrections without taking the value of ε_0 into account. It is a very well known fact in the Casimir physics that the small a /low T behavior of the Casimir interaction is governed by the high-frequency behavior of reflection coefficients, while in the opposite limit the zeroth Matsubara frequency becomes increasingly important. This is roughly related to the presence of the damping factor e^{2aq_n} in the Lifshitz formula (36) and to the temperature dependence of the spacing in the Matsubara sum. Although the reflection coefficients are related to ε^l and ε^t through complicated formulas (38), one can deduce some qualitative results by looking at the properties of $\varepsilon^{l,t}$ which we discussed in the previous section. The zero-frequency positive peak in $\varepsilon^{l,t}$ effectively increases optical density of the material and thus leads to an increase of the Casimir pressure at large a and high T . The negative tail which becomes more visible at higher frequencies leads to a decrease of the Casimir pressure in the small a and low T regions. This is exactly what we see at Figs. 2 and 3. As another check of our qualitative understanding it is useful to consider the dependence of critical temperature T_c (at which $P = P_d$) on the mass and chemical potential, see Fig. 4. It is clear on the basis of our arguments above, that the higher is the peak in $\varepsilon^{l,t}$, the smaller T_c has to be. From the expression (34), we see that as long as $\mu < m$ the increase of μ leads to strong enhancement of ε^l due an exponential factor. For $\mu > m$ the dependence of ε^l on μ is weaker, as follows from Eq. (35). These two regions are clearly seen at Fig. 4(b). The dependence on m is a bit more complicated. Actually, the increase of the mass gap leads to a decrease of all quantum corrections, both in the ‘‘peak’’ and in the ‘‘tail’’. For $T \ll m$ suppression of the ‘‘peak’’ is exponential, see Eq. (34) and is more important than suppression of the ‘‘tail’’. For lower values of m the ‘‘tail’’ suppression wins. This latter effect cannot be confirmed by our analytic formulas, but it is clearly seen at Fig. 4(a).

Let us now discuss the contribution of the zero Matsubara frequency term in Eq. (36) to the Casimir pressure. By comparing the graphs in Figs. 5(a) and 5(b) we observe that practically the whole dependence of the Casimir pressure on μ and T is due to this term. (A similar picture occurs until very

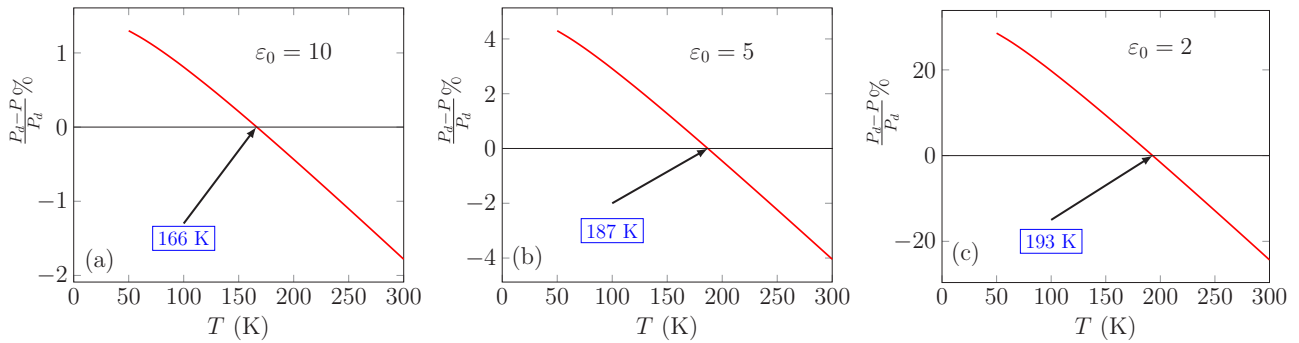


FIG. 3. The relative difference in percent $(P_d - P)/P_d\%$. The values $m = 0.01$ eV, $a = 200$ nm, and $\mu = 0$ eV are used. ϵ_0 is taken to be 10, 5, and 2 in (a), (b) and (c), respectively.

small distances.) The usual dominance of the zero Matsubara frequency in the Casimir pressure is enhanced in our case by strong dependence of the “peak” in dielectric functions on both T and μ (while the “tail” practically does not depend on these parameters). A similar effect has been observed in the Casimir interaction of graphene [10,35]. One may conjecture that this is a general property of Dirac materials. This is very remarkable fact which considerably simplifies numerical calculations. For $\mu = 0$, and for small values of μ as well, there is no dependence of P on T for low temperature. This can be traced back to the strong temperature suppression in Eq. (34). There is no such suppression for $\mu > m$, see (35). The T dependence of pressure for $\mu > m$ is caused by an $O(T)$ correction which is not shown in Eq. (35). The behavior of the Casimir pressure at finite T cannot be fully understood by asymptotic formulas. Thus, we have to rely on the numerics which shows that P increases considerably with the increase of T or μ .

V. CONCLUSIONS

The purpose of this paper was to compute the bulk dielectric functions for Dirac materials at imaginary frequencies and to study their effect on the Casimir interaction. Let us summarize briefly our findings. The structure of dielectric functions was quite simple: a strong and sharp positive peak near the zero frequency and a long smooth negative tail, see Fig. 1. This structure causes an increase of the Casimir pressure at large separations and high temperatures, and a decrease at small separation and low temperature, as compared to the interaction of dielectrics with a constant dielectric

permittivity ϵ_0 . Other properties of the Casimir pressure also got nice qualitative explanation through the properties of quantum corrections to dielectric functions. We found that the dependence of the Casimir energy on temperature and chemical potential is almost entirely due to the contribution from the zeroth Matsubara term in the Lifshitz sum. This fact leads to great simplifications in the numerics. We like to stress that the effects of quantum corrections to dielectric functions are very well seen in the Casimir interaction, as well as the influence of mass gap and chemical potential.

The publications on the Casimir interaction of Dirac and similar materials have been reviewed in Refs. [4,5]. Almost all of these papers did not consider the effects of quantum Dirac fermions in the bulk. There are exceptions, however. Reference [8] considered lattice fermions in various dimensions, but the Casimir energy computed there was a function of the size of samples (rather than of the distance between samples, as in our work) and was caused by vacuum fluctuations of fermions (rather than by an interaction of quantum fermions with quantum photons as in our work). The Casimir interaction of Weyl semimetals was studied in Refs. [6,7,36]. It should be possible to compare some limiting cases of these papers to our work. However, the authors of Refs. [7,36] used only the anomalous (antisymmetric) part of the polarization tensor (which is absent in our case) and neglected the symmetric part. The study of Ref. [6] was based on the conductivity tensor calculated within the Kubo approach, which made all the quantities dependent on a cutoff parameter. The role of this parameter is still unclear. The QFT method used here does not provide any additional parameters in the description of the system. Reference [6] studied the case $m = 0$ and used the absolute value of vector b describing the separation of Weyl points in the momentum space as a scale parameter. Thus, the limit $b \rightarrow 0$ is tricky. All in all, Ref. [6] and the present work studied completely different ranges of physical parameters by different methods.

At the same time, it would be very interesting to redo the calculations of Ref. [6] within the QFT approach advocated in the present paper. The presence of field b leads to a possibility of Casimir repulsion. By looking at our results one may suggest that the repulsion is more likely to happen at small separation where the attractive interaction is weaker, see Fig. 2. However, without precise calculations this prediction should be taken with a grain of salt.

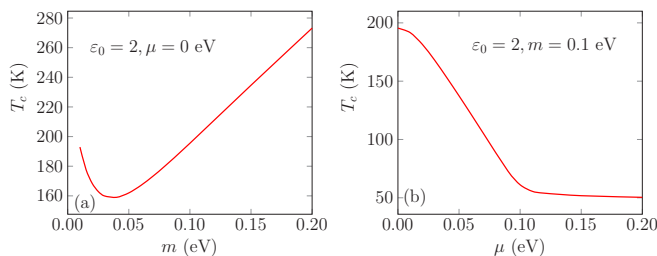


FIG. 4. The dependence of critical temperature T_c on the mass gap m (a) and on the chemical potential μ (b). The values $\epsilon_0 = 2$, $a = 200$ nm are used.

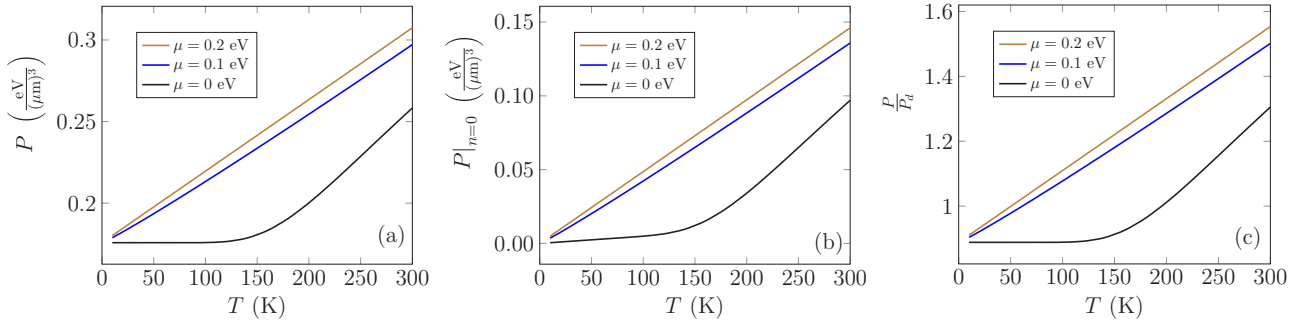


FIG. 5. The plots of temperature dependence of (a) the Casimir pressure, (b) the contribution of zero Matsubara term to the Casimir pressure, and (c) the relative the Casimir pressure for $\epsilon_0 = 2$, $m = 0.1$ eV, $a = 200$ nm, and three different values of the chemical potential $\mu = 0, 0.1, 0.2$ eV.

The limit $m \rightarrow 0$ (Dirac semimetals) cannot be taken in our formulas immediately. The polarization tensor at $T = 0 = \mu$ diverges in this limit which is the usual zero mass singularity of QFT. This singularity can be easily avoided by changing the normalization point. Also, in this work we used a dielectric with constant ϵ as a reference material which is not a natural choice in the case of semimetals. Both problems are technical and easy to solve, but one has to redo all calculations reported above.

In this work, boundary contributions to the polarization tensor have been neglected. To take them properly into account, one has to extend the results of Refs. [23,30] to the case of nonzero temperature and chemical potential. We hope to address this problem in a future publication. The present work also did not consider possible contributions to the dielectric functions from other sources (from phonons, for example). Taking these contributions into account is also a task for some future work when we shall consider particular materials.

ACKNOWLEDGMENTS

We are grateful to M. Kurkov for fruitful discussions. This work was supported in part by Project No. 2016/03319-6 of FAPESP, by Grants No. 305594/2019-2 and No. 428951/2018-0 of the CNPq. D.V. was supported by the Tomsk State University Competitiveness Improvement Program. N.K. was supported in part by Project No. 2019/10719-9 of FAPESP and by the RFBR Project No. 19-02-00496-a.

APPENDIX: COMPUTATION OF THE POLARIZATION TENSOR

Here we sketch the computation of polarization tensor $\widehat{\Pi}^{\mu\nu}$ for unit Fermi velocity, $v_F = 1$. The formalism which we apply here is rather standard, see Ref. [37]. Exactly the same methods were used in Refs. [35,38,39], see also Ref. [40], to compute the polarization tensor in graphene for nonzero temperature and chemical potential.

After computing the traces of γ matrices in Eq. (8) we arrive at the following expression [see notations below Eq. (10)]:

$$\widehat{\Pi}^x(p) = -4e^2 T \sum_{l=-\infty}^{\infty} \int \frac{d^3 \vec{k}}{(2\pi)^3} \frac{Z^x}{N}. \quad (\text{A1})$$

Here,

$$Z^{00} = m^2 - (k_4 - i\mu)(k_4 - i\mu + ip_0) + \vec{k}(\vec{k} - \vec{p}), \quad (\text{A2})$$

$$Z^{tr} = 4m^2 + 2(k_4 - i\mu)(k_4 - i\mu + ip_0) + 2\vec{k}(\vec{k} - \vec{p}), \quad (\text{A3})$$

$$N = [(k_4 - i\mu)^2 + E_k^2][(k_4 - i\mu + ip_0)^2 + E_{k-p}^2], \quad (\text{A4})$$

with $k_0 = ik_4 = 2\pi T(l + \frac{1}{2})$, $E_k = \sqrt{\vec{k}^2 + m^2}$ and $E_{k-p} = \sqrt{(\vec{k} - \vec{p})^2 + m^2}$.

We express the sum over Matsubara frequencies through a contour integral

$$\widehat{\Pi}^x(p) = 4e^2 \oint_{\gamma} \frac{dk_4}{1 + e^{i\frac{k_4}{T}}} \int \frac{d^3 \vec{k}}{(2\pi)^4} \frac{Z^x}{N}. \quad (\text{A5})$$

The contour $\gamma = \gamma_1 \cup \gamma_2$ consists of two parts which are depicted in Fig. 6.

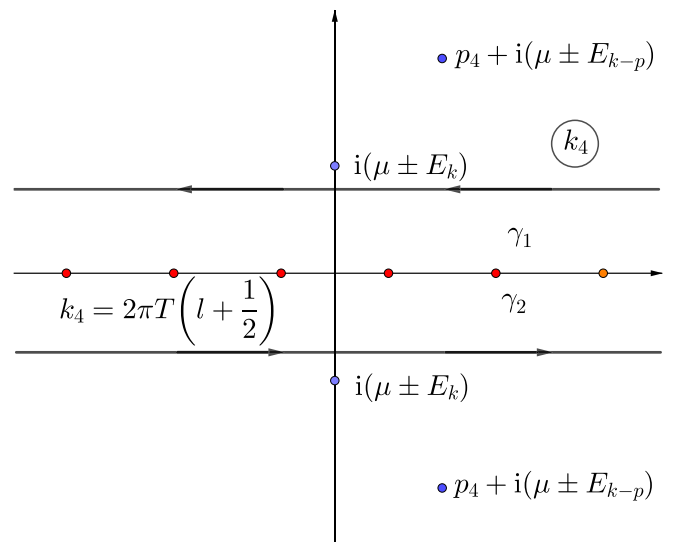


FIG. 6. The integration contour $\gamma = \gamma_1 \cup \gamma_2$ in the complex k_4 plane, see Eq. (A5). Here we also marked the positions of poles of the integrand. Depending on the signs of $\mu \pm E_k$ and of $\mu \pm E_{k-p}$ some poles may appear either in the upper or in the lower half-plane. Both possibilities are depicted.

On the upper part γ_1 of the contour we use the identity

$$\frac{1}{1 + e^{\frac{k_4}{T}}} = 1 - \frac{1}{1 + e^{-i\frac{k_4}{T}}}. \quad (\text{A6})$$

Contribution of the first (constant) term in Eq. (A6) reads

$$\widehat{\Pi}_1^x(p) = 4e^2 \int_{+\infty}^{-\infty} dk_4 \int \frac{d^3\vec{k}}{(2\pi)^4} \frac{Z^x}{N}. \quad (\text{A7})$$

With just the second term in Eq. (A6) present under the integral, the integration contour γ_1 can be closed upwards. The contour γ_2 can be closed downwards. The integration over k_4 is done by computing the residues. After some long but otherwise straightforward algebra, we obtain the rest of $\widehat{\Pi}_T = \widehat{\Pi} - \widehat{\Pi}_1$:

$$\widehat{\Pi}_T^x(p) = \frac{e^2}{4\pi^3} \int \frac{d^3\vec{k}}{E_k} \left\{ \frac{Z^x[k_4 = i(\mu + E_k)]}{E_{k-p}^2 - (p_0 + E_k)^2} [n_\mu + n_{-\mu} - \theta(\mu - E_k) - \theta(-\mu - E_k)] \right.$$

$$\left. \widehat{\Pi}_0^x(p) = -\frac{e^2}{4\pi^3} \int d^3\vec{k} \left\{ \int_{-\infty}^{+\infty} \frac{dk_4}{\pi} \frac{Z^x}{N} + \frac{1}{E_k} \left[\frac{Z^x[k_4 = i(\mu + E_k)]}{E_{k-p}^2 - (ip_4 + E_k)^2} + \frac{Z^x[k_4 = i(\mu - E_k)]}{E_{k-p}^2 - (ip_4 - E_k)^2} \right] \theta(\mu^2 - E_k^2) \right\}, \quad (\text{A10})$$

$$\widehat{\Pi}_{T,\mu}^x(p) = \frac{e^2}{4\pi^3} \int \frac{d^3\vec{k}}{E_k} \left\{ \frac{Z^x[k_4 = i(\mu + E_k)]}{E_{k-p}^2 - (ip_4 + E_k)^2} + \frac{Z^x[k_4 = i(\mu - E_k)]}{E_{k-p}^2 - (ip_4 - E_k)^2} \right\} (n_\mu + n_{-\mu}). \quad (\text{A11})$$

It remains to integrate over k_4 in (A10) and perform the angular integration in $d^3\vec{k}$ in both formulas above to obtain Eqs. (11)–(15) of the main text.

$$\left. \begin{aligned} &+ \frac{Z^x[k_4 = i(\mu - E_k)]}{E_{k-p}^2 - (p_0 - E_k)^2} [n_{-\mu} + n_\mu - \theta(\mu - E_k) \\ &- \theta(-\mu - E_k)] \end{aligned} \right\}. \quad (\text{A8})$$

Here

$$n_{\pm\mu} = \frac{1}{1 + e^{\frac{E_k \pm \mu}{T}}} \quad (\text{A9})$$

is the Boltzmann factor. We remind the reader that $p_0 = ip_4 = 2\pi inT = i\xi_n$ is an imaginary bosonic Matsubara frequency. Thus, $n_{\mu \pm p_0} = n_\mu$.

It is useful to take the terms containing step functions θ out of the expressions (A8) and combine them with $\widehat{\Pi}_1$. The reshuffled contributions to polarization tensor read

-
- [1] X. L. Qi and S. C. Zhang, Topological insulators and superconductors, *Rev. Mod. Phys.* **83**, 1057 (2011).
- [2] M. Z. Hasan and C. L. Kane, Topological Insulators, *Rev. Mod. Phys.* **82**, 3045 (2010).
- [3] M. Bordag, G. L. Klimchitskaya, U. Mohideen, and V. M. Mostepanenko, *Advances in the Casimir effect*, Int. Ser. Monogr. Phys., Vol. 145 (Oxford University Press, Oxford, UK, 2009), pp. 1–768.
- [4] L. Woods, D. Dalvit, A. Tkatchenko, P. Rodriguez-Lopez, A. Rodriguez, and R. Podgornik, Materials perspective on Casimir and van der Waals interactions, *Rev. Mod. Phys.* **88**, 045003 (2016).
- [5] B.-S. Lu, The Casimir effect in topological matter, *Universe* **7**, 237 (2021).
- [6] P. Rodriguez-Lopez, A. Popescu, I. Fialkovsky, N. Khusnutdinov, and L. M. Woods, Signatures of complex optical response in Casimir interactions of type I and II Weyl semimetals, *Commun. Mater.* **1**, 14 (2020).
- [7] M. B. Farias, A. A. Zyuzin, and T. L. Schmidt, Casimir force between Weyl semimetals in a chiral medium, *Phys. Rev. B* **101**, 235446 (2020).
- [8] T. Ishikawa, K. Nakayama, and K. Suzuki, Lattice-fermionic Casimir effect and topological insulators, *Phys. Rev. Research* **3**, 023201 (2021).
- [9] M. Bordag, I. V. Fialkovsky, D. M. Gitman, and D. V. Vassilevich, Casimir interaction between a perfect conductor and graphene described by the Dirac model, *Phys. Rev. B* **80**, 245406 (2009).
- [10] I. V. Fialkovsky, V. N. Marachevsky, and D. V. Vassilevich, Finite temperature Casimir effect for graphene, *Phys. Rev. B* **84**, 035446 (2011).
- [11] A. A. Banishev, H. Wen, J. Xu, R. K. Kawakami, G. L. Klimchitskaya, V. M. Mostepanenko, and U. Mohideen, Measuring the Casimir force gradient from graphene on a SiO₂ substrate, *Phys. Rev. B* **87**, 205433 (2013).
- [12] G. L. Klimchitskaya, U. Mohideen, and V. M. Mostepanenko, Theory of the Casimir interaction from graphene-coated substrates using the polarization tensor and comparison with experiment, *Phys. Rev. B* **89**, 115419 (2014).
- [13] M. Liu, Y. Zhang, G. L. Klimchitskaya, V. M. Mostepanenko, and U. Mohideen, Demonstration of an Unusual Thermal Effect in the Casimir Force from Graphene, *Phys. Rev. Lett.* **126**, 206802 (2021).
- [14] G. L. Klimchitskaya and V. M. Mostepanenko, An alternative response to the off-shell quantum fluctuations: A step forward in resolution of the Casimir puzzle, *Eur. Phys. J.* **C80**, 900 (2020).
- [15] G. L. Klimchitskaya and V. M. Mostepanenko, Casimir entropy and nonlocal response functions to the off-shell quantum fluctuations, *Phys. Rev. D* **103**, 096007 (2021).
- [16] A. A. Abrikosov and S. D. Beneslavskii, Possible existence of substances intermediate between

- metals and dielectric, *Sov. Phys. JETP* **32**, 699 (1971).
- [17] R. E. Throckmorton, J. Hofmann, E. Barnes, and S. Das Sarma, Many-body effects and ultraviolet renormalization in three-dimensional Dirac materials, *Phys. Rev. B* **92**, 115101 (2015).
- [18] J. Zhou, H.-R. Chang, and D. Xiao, Plasmon mode as a detection of the chiral anomaly in Weyl semimetals, *Phys. Rev. B* **91**, 035114 (2015).
- [19] J. Hofmann and S. Das Sarma, Plasmon signature in Dirac-Weyl liquids, *Phys. Rev. B* **91**, 241108(R) (2015).
- [20] M. Lv and S.-C. Zhang, Dielectric functions, Friedel oscillations and plasmons in Weyl semimetals, *Int. J. Mod. Phys. B* **27**, 1350177 (2013).
- [21] J. Lindhard, On the properties of a gas of charged particles, *Dan. Mat. Fys. Medd.* **28**, 2 (1954).
- [22] M. Bordag and I. Pirozhenko, Dispersion forces between fields confined to half spaces, *Symmetry* **10**, 74 (2018).
- [23] I. Fialkovsky, M. Kurkov, and D. Vassilevich, Quantum Dirac fermions in a half-space and their interaction with an electromagnetic field, *Phys. Rev. D* **100**, 045026 (2019).
- [24] H. Isobe and N. Nagaosa, Theory of quantum critical phenomenon in topological insulator - (3+1)D quantum electrodynamics in solids, *Phys. Rev. B* **86**, 165127 (2012).
- [25] B. Roy, V. Juricic, and I. F. Herbut, Emergent Lorentz symmetry near fermionic quantum critical points in two and three dimensions, *J. High Energy Phys.* **04** (2016) 18.
- [26] O. Pozo, Y. Ferreira, and M. A. H. Vozmediano, Anisotropic fixed points in Dirac and Weyl semimetals, *Phys. Rev. B* **98**, 115122 (2018).
- [27] M. N. Chernodub and M. A. H. Vozmediano, Direct measurement of a beta function and an indirect check of the Schwinger effect near the boundary in Dirac-Weyl semimetals, *Phys. Rev. Research* **1**, 032002(R) (2019).
- [28] L. D. Landau, E. M. Lifshitz, and L. P. Pitaevskii, *Electrodynamics of continuous media* (Pergamon, Oxford, 1984).
- [29] N. Khusnutdinov and N. Emelianova, Low-temperature expansion of the Casimir-Polder free energy for an atom interacting with a conductive plane, *Int. J. Mod. Phys. A* **34**, 1950008 (2019).
- [30] M. Kurkov and D. Vassilevich, How Many Surface Modes Does One See on the Boundary of a Dirac Material? *Phys. Rev. Lett.* **124**, 176802 (2020).
- [31] G. E. H. Reuter and E. H. Sondheimer, The theory of anomalous skin effect in metals, *Proc. R. Soc. London, Ser. A* **195**, 336 (1948).
- [32] V. P. Silin and E. P. Fetisov, Electromagnetic properties of a relativistic plasma, *Sov. Phys. JETP* **14**, 115 (1962).
- [33] K. L. Kliewer and R. Fuchs, Anomalous skin effect for specular electron scattering and optical experiments at non-normal angles of incidence, *Phys. Rev.* **172**, 607 (1968).
- [34] R. Esquivel and V. B. Svetovoy, Correction to the Casimir force due to the anomalous skin effect, *Phys. Rev. A* **69**, 062102 (2004).
- [35] M. Bordag, I. Fialkovskiy, and D. Vassilevich, Enhanced Casimir effect for doped graphene, *Phys. Rev. B* **93**, 075414 (2016).
- [36] J. H. Wilson, A. A. Allocca, and V. Galitski, Repulsive Casimir force between Weyl semimetals, *Phys. Rev. B* **91**, 235115 (2015); [arXiv:1501.07659](https://arxiv.org/abs/1501.07659) [cond-mat.mes-hall].
- [37] E. V. Shuryak, Quantum chromodynamics and the theory of superdense matter, *Phys. Rep.* **61**, 71 (1980).
- [38] M. Bordag, G. L. Klimchitskaya, V. M. Mostepanenko, and V. M. Petrov, Quantum field theoretical description for the reflectivity of graphene, *Phys. Rev. D* **91**, 045037 (2015) [Erratum: **93**, 089907(E) (2016)].
- [39] M. Bordag and I. G. Pirozhenko, Surface plasmons for doped graphene, *Phys. Rev. D* **91**, 085038 (2015).
- [40] H. Falomir, E. Muñoz, M. Loewe, and R. Zamora, Optical Conductivity in an effective model for Graphene: Finite temperature corrections, *J. Phys. A* **53**, 015401 (2020).